Bed stability in unconfined gravel bed mountain streams: With implications for salmon spawning viability in future climates

Jim McKean[1] and Daniele Tonina[2]

Received 11 October 2012; revised 31 May 2013; accepted 7 June 2013; published 18 July 2013.

[1] Incubating eggs of autumn-spawning Chinook salmon (*Oncorhynchus tshawytscha*) could be at risk of midwinter high flows and substrate scour in a changing climate. A high-spatial-resolution multidimensional hydrodynamics model was used to assess the degree of scour risk in low-gradient unconfined gravel bed channels that are the favored environment for autumn-spawning salmon in mountain watersheds such as the Middle Fork Salmon River (MFSR), Idaho. In one of the most important MFSR spawning tributaries, near-bed shear stresses were relatively low at all discharges from base flows to 300% of bankfull. The highest stresses were found only in small areas of the central flow core and not at spawning sites. Median shear stresses did not increase in overbank flow conditions because poor channel confinement released the excess water into adjacent floodplains. Channel and floodplain topography, rather than discharge, control the maximum near-bed shear stresses. Over the modeled range of discharges, ~2% of the total surface area of the main stem channel bed was predicted to be mobile. Even in known spawning areas, where shear stresses are higher, ≤20% of the spawning surface area was mobile during overbank flows with a 2 year recurrence interval. Field measurements of little gravel transport during flows that were 93% of bankfull support the numerical model predictions. Regardless of some uncertainty in future climates in these watersheds, there appears to be relatively limited risk of extensive scour at salmon spawning sites in any likely hydrologic regimes.

Citation: McKean, J., and D. Tonina (2013), Bed stability in unconfined gravel bed mountain streams: With implications for salmon spawning viability in future climates, *J. Geophys. Res. Earth Surf.*, *118*, 1227–1240, doi:10.1002/jgrf.20092.

1. Introduction

[2] Motion of sediment in a gravel bed channel is normally considered to begin at a critical flow condition in which the near-bed shear stress just exceeds the threshold value for particle entrainment. However, mobility of the streambed surface varies both spatially and temporally. At lower flows, only a small portion of the bed or only the smaller grains may be mobile [e.g., *Jackson and Beschta*, 1982; *Wilcock and McArdell*, 1993; *Haschenburger and Wilcock*, 2003]. As flows increase, more of the bed and larger particles begin to move until full mobility of all particles is achieved everywhere [*Carling*, 1988]. Resistance to particle motion is normally described by some form of an empirical nondimensional threshold shear stress, such as the critical Shields stress:

$$\tau^*_{c,i} = \frac{\tau_{c,i}}{(\rho_s - \rho_w)\, g\, d_i} \tag{1}$$

[3] Here $\tau_{c,i}$ is the critical shear stress for some particular grain size (d_i), ρ_s and ρ_w are the bulk densities of the sediment and water, respectively, and g is the gravitational acceleration. There has been much discussion of the Shields stress and what values it might take in different fluvial situations (see reviews by, among others, *Richards* [1990] and *Buffington and Montgomery* [1997]). In 24 gravel bed streams in the Rocky Mountains, *Andrews* [1984] reported that the threshold of particle motion was reached when $\tau^*_{c,i} \approx 0.046$. *Lisle et al.* [2000], in a study of six natural gravel bed channels, used categories of (a) a stable bed when $\tau^*_{c,i} < 0.03$, (b) partial bed mobility when $0.03 < \tau^*_{c,i} < 0.06$, and (c) full mobility if $\tau^*_{c,i} > 0.06$ or about twice the stress at initial motion. Many investigators have also observed that sediment mobility and bed load transport increase greatly, often to a state of full bed and grain mobility, at flows near bankfull discharge [e.g., *Li et al.*, 1976; *Parker*, 1979; *Jackson and Beschta*, 1982; *Andrews*, 1983, 1984; *Andrews and Erman*, 1986; *Carling*, 1988; *Richards*, 1990; *Ryan and Troendle*, 1996; *Ryan and Emmett*, 2002; *Haschenburger and Wilcock*, 2003; *King et al.*, 2004; *Torizzo and Pitlick*, 2004; *Mueller et al.*, 2005].

[4] In many mountain rivers in western North America, the annual hydrograph is dominated by the spring-early summer

[1]Rocky Mountain Research Station, US Forest Service, Boise, Idaho, USA.
[2]Center for Ecohydraulics Research, Department of Civil Engineering, University of Idaho, Boise, Idaho, USA.

Corresponding author: J. McKean, Rocky Mountain Research Station, US Forest Service, 322 E. Front St., Ste. 401, Boise, ID 83702, USA. (jmckean@fs.fed.us)

©2013. American Geophysical Union. All Rights Reserved.
2169-9003/13/10.1002/jgrf.20092

snowmelt, which reliably produces the majority of the annual flow volume and often also the largest peak daily flows [*Jarrett*, 1990; *Hauer et al*., 1997; *Hamlet et al*., 2005; *Bales et al*., 2006]. Whereas single storms, such as rain-on-snow events or summer thunderstorms, infrequently cause high short-term stream runoff, the annual snowmelt can produce as large, or larger, discharges and often endures for several weeks. Thus, annually, the highest shear stresses and the majority of sediment transport and bed motion tend to occur during snowmelt runoff. In western North America, this characteristic is accentuated in streams in inland mountains with a nonmaritime climate and in watersheds that lie at higher elevations where a greater portion of the total precipitation occurs as snow and winter discharges are relatively low [e.g., *Jarrett*, 1990; *Hauer et al*., 1997; *Beebee and Manga*, 2004; *Stewart et al*., 2004; *Torizzo and Pitlick*, 2004; *Mote et al*., 2005].

[5] Large flow events can dramatically alter the physical habitat of stream ecosystems and strongly affect in-stream biodiversity [e.g., *Kondolf et al*., 1991; *Naiman et al*., 2008]. However, when spatial or temporal patterns in the flow regime are somewhat predictable, such as the annual spring snowmelt discharge peak in mountain streams, aquatic species have the opportunity to adapt and evolve successful responsive life histories and strategies to avoid, cope with, or even exploit these extreme events [*Hauer et al*., 1997; *Gasith and Resh*, 1999; *Naiman et al*., 2008]. For example, reproduction is often timed to minimize exposure of young to predictable high flows and then allow juveniles to take advantage of improving recessional limb conditions with lower velocities, higher productivity, and greater food availability [*Yarnell et al*., 2010]. Some natural variability in timing, magnitude, and duration of extreme events can be tolerated and may even lead to higher biodiversity [*Naiman et al*., 2008; *Rieman and Isaak*, 2010], but events outside the range of adaption can lead to poor species success [*Kondolf et al*., 1991; *Yarnell et al*., 2010].

[6] The iconic anadromous Chinook salmon has adapted its reproductive life stage to accommodate a relatively predictable annual hydrograph in many snowmelt-dominated western North American mountain streams [e.g., *Quinn* 2005; *Waples et al*., 2008]. These fish famously use the channel bed substrate as an egg-incubating medium and construct a nest, or "redd," in streambed gravels whose matrix structural integrity is essential for successful development of embryos and alevins [*Burner*, 1951]. In mountain streams, salmon reproduction is timed and designed to accommodate the snowmelt peak flow period and minimize the possibility of gravel movement during incubation. For example, autumn-spawning Chinook have evolved to incubate their eggs during winter low flows and the juveniles emerge from the gravels before the spring snowmelt period [*Quinn*, 2005]. Another successful strategy is to bury the eggs deeper than the normal scour depth [e.g., *DeVries*, 1997; *Montgomery et al*., 1996].

[7] Several previous studies have raised concerns about the possibility of high flows scouring fish nest sites during an incubation period, with obvious harmful effects on population dynamics [e.g., *Seegrist and Gard*, 1972; *Meehan*, 1974; *Holtby and Healy*, 1986; *Lisle*, 1989; *Lapointe et al*., 2000; *Schuett-Hames et al*., 2000; *Clark et al*., 2001; *Tonina et al*., 2008; *May et al*., 2009]. Recently, some have also suggested that new flow regimes in future climates may force more frequent bed scour during incubation [*Hauer et al*., 1997; *Battin et al*., 2007] as a result of earlier snowmelt or increased winter rain-on-snow runoff events [e.g., *Lettenmaier and Gan*, 1990; *Pupacko*, 1993; *Dettinger and Cayan*, 1995; *Stewart et al*., 2004, 2005; *Regonda et al*., 2005; *Maurer et al*., 2007; *Stewart*, 2009]. However, there appear to have been few mechanistic studies of this potentially serious ecological issue in western North American rivers. A notable exception is the investigation of *May et al*. [2009] who explored the risk of sediment scour and deposition at salmon redds in a large regulated river in Northern California. Using a combination of numerical flow modeling and field observations, they found that redds were preferentially located in coarse substrate near the banks and unlikely to be scoured in high-flow reservoir releases, during which greater bed shear stresses and mobility were concentrated in a flow core closer to the middle of the channel.

[8] In this study, we tested the potential for midwinter scour of Chinook salmon nesting sites during natural high flows in unregulated, low-gradient, unconfined gravel bed streams in high-elevation snowmelt-dominated watersheds. We investigated the tributaries of the Middle Fork Salmon River (MFSR), Idaho, because of their importance to the spawning of this threatened fish species. It is difficult to accurately predict future changes in the amount and timing of snowmelt runoff or the magnitude, frequency, and timing of rain or rain-on-snow discharge events [*Beniston et al*., 2003; *Mote et al*., 2003; *Battin et al*., 2007; *Harpold et al*., 2012]. Therefore, we explored the sensitivities of shear stress and bed mobility to a range of discharges from base flows to near-bankfull and overbank flows representing some of the largest discharges that could likely result from future severe winter climate conditions in the study streams. We used a calibrated multidimensional fluid dynamics model to predict local near-bed shear stresses. We then compared the predicted near-bed stresses to critical values for initial motion of streambed material defined from field-measured substrate size ranges.

2. Study Area

[9] The MFSR is the largest and most important anadromous fish-bearing stream in the Salmon River drainage, which, in turn, is one of the most important rivers in the Columbia River drainage for Chinook salmon production [*Andrews and Everson*, 1988]. The main stem MFSR flows north-northeastward for about 200 km through the Frank Church–River of No Return Wilderness Area in central Idaho (Figure 1). This main stem river is used primarily as a travel corridor by anadromous fish moving between the ocean and spawning/rearing habitat in meandering gravel bed tributary channels [*Thurow*, 2000; *Isaak and Thurow*, 2006]. For example, during a 3 year period of intensive monitoring of MFSR Chinook salmon spawning, *Thurow* [2000] found 99% of redds constructed in tributaries, with the largest concentrations in the Bear Valley, Elk, and Marsh Creeks drainages. Over much of its course, the main MFSR is confined in deep canyons with steep sidewalls, but the upper reaches of many of its tributaries flow through broad gentle valleys that often were formed by glaciers or by outwash debris from up-valley glacial sources [*Fisher et al*., 1992; *Meyer and Leidecker*, 1999]. Thus, in the MFSR watershed, salmon spawning is concentrated in a specific subset of channel morphologies.

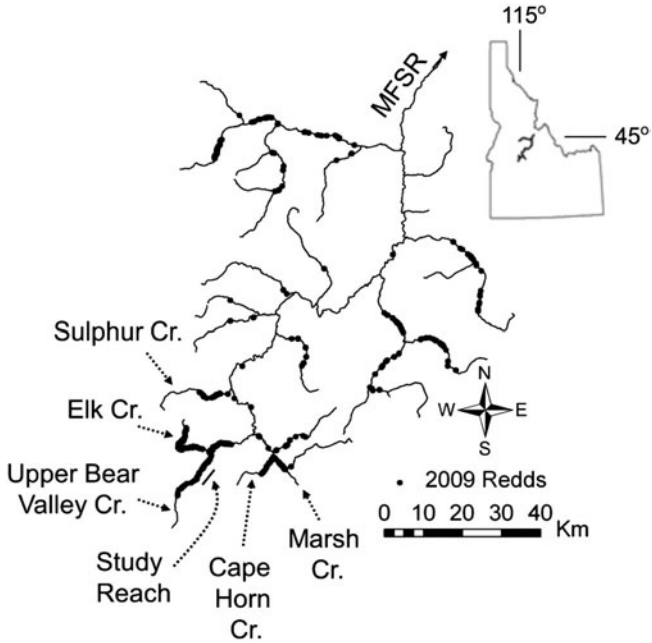

Figure 1. Middle Fork Salmon River (MFSR) and primary tributaries, central Idaho, USA. Distribution of Chinook salmon nesting sites (redds) in 2009 shown in black dots (584 total in watershed; 101 (17%) in Elk Creek; 130 (22%) in upper Bear Valley Creek; 49 (8%) in Marsh Cr.); 27 (5%) in Sulphur Creek.; and 29 (5%) in Cape Horn Creek).

[10] A 1.6 km reach of upper Bear Valley Creek was selected to represent spawning habitat in headwater unconfined low-gradient streams (Figure 1). Upper Bear Valley Creek is a meandering pool-riffle channel that flows across a wide, gently sloping valley formed in glacial outwash sediments [*Schmidt and Mackin*, 1970; *McKean et al*., 2008]. The study reach is a gravel bed channel, 12–15 m wide and <2.5 m deep (Figure 2). The surface substrate median grain size for spawning sites within the model reach is 35 mm, whereas the median grain size for the whole of upper Bear Valley Creek, which includes some coarser plane bed reaches, is 52 mm (Figure 3). The stream is armored with a ratio of surface d_{50} to subsurface d_{50} of approximately 2.5. The average gradient over the model domain is 0.3% with local gradients as high as 0.6% over 100 m distances. A rating curve was established from a temporary staff gauge at the study reach with flow observations made over a range from 1.1 to 6.2 $m^3 s^{-1}$. These measurements and topographic observations indicate that bankfull flow is 6.7 $m^3 s^{-1}$.

[11] Upper Bear Valley Creek is a high-altitude stream with an average elevation of about 2000 m. The watershed mean precipitation is about 78 cm yr^{-1}, most of which occurs as snow with some minor contributions from occasional midsummer thunderstorms. The annual runoff hydrograph is dominated by the spring snowmelt from mid-April to mid-June (Figure 4). Historically, spring overbank flooding of the low-gradient meadows is sustained for approximately 6–8 weeks, or 10–15% of each year (Figure 4), depending on the size of the winter snow accumulation and the intensity and duration of warmer air temperatures that cause snowmelt. Rain or rain-on-snow events have a much smaller duration, causing floods of 1 to a few days. During overbank flooding in these streams, the width of flow increases significantly, while the depth and shear stress increase much less. These general hydrologic characteristics of Bear Valley Creek are similar to those of many other headwater tributary streams in the MFSR [*King et al*., 2004] and the main Salmon River drainages [*Emmett*, 1975].

[12] The direct sediment supply from hillslopes appears low in Bear Valley Creek due to its isolation from the valley sides by the wide low-gradient meadow surfaces. The majority of sediment supplied to the channel is likely from localized bank erosion that delivers sand and gravel. By direct observation, the subreach-scale morphology of the channel is essentially constant over annual and even multiyear periods. For example, local topographic changes between 2004 and 2007 were evaluated in a 10 km reach of upper Bear Valley Creek by computing the difference between high-resolution digital elevation models (DEMs) constructed from bathymetric lidar surveys in those years. Ground surveys of three ~150 m long reaches were also repeated in 2004, 2006, and 2007. The overall channel morphology did not change during this interval and local bed elevations varied <10 cm. The positions of spawning areas were very persistent, and frequently, prior year redds were observed that had not changed shape during the intervening snowmelt peak flows.

[13] Local Chinook salmon have evolved their spawning and rearing life stages around the annual runoff pattern (Figure 4). Each year, returning adult fish arrive in July and then spawn in August-September. Incubation takes place over the winter months while flows are historically very low and little sediment transport occurs. Eggs hatch and fry emerge from the streambed in February-March, just prior to the yearly high flows. Any change in the normal annual hydrograph that involved high flows and bed mobility during the winter incubation, whether caused by earlier snowmelt, rain-on-snow, or rainstorms, could be detrimental to spawning success. As snowmelt progresses during May-June, discharges increase beyond bankfull and many of the fry escape the high-velocity flows by dispersing into flooded off-channel areas in adjacent low-gradient meadows. The young fish occupy these channel and off-channel habitats for 1–2 years and then out-migrate down the Middle Fork Salmon drainage to spend about 5 years in the ocean prior to returning as spawning adults.

Figure 2. Field conditions. Measuring discharge in upper Bear Valley Creek at an intermediate flow stage. View is downstream.

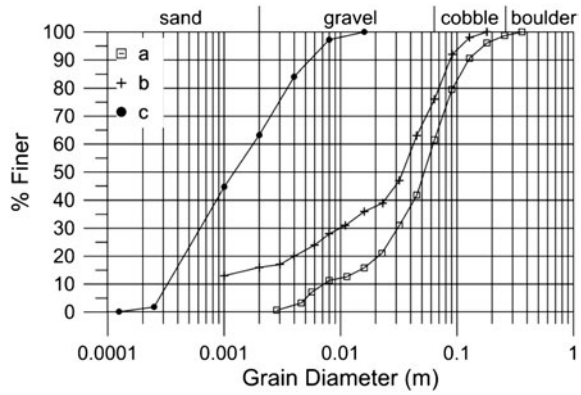

Figure 3. Grain size curves from field samples: pebble count–overall bed average (open squares), pebble count–spawning areas only (crosses), and bed load transport sample (solid circles).

3. Numerical Model

[14] We used the Flow and Sediment Transport Morphological Evolution of Channels (FaSTMECH) model [*Nelson et al*., 2003; *Nelson and Smith*, 1989; *Nelson and McDonald*, 1997] to predict water surface elevation, flow depth and velocity, shear stress, and nondimensional Shields stress near the channel bed. FaSTMECH is a steady flow, hydrostatic model that considers turbulence by employing an isotropic eddy viscosity to relate Reynolds stress to shear [*Nelson et al*., 2003]. Flow resistance is described by a drag coefficient that varies spatially as

$$C_d = \left[\frac{1}{h}\int_{z_o}^{h} f(z, z_o)\, dz\right]^{-2} \tag{2}$$

[15] Here h is the flow depth, z is the height above the streambed, and z_o defines the depth at which velocity is equal to zero (no-slip condition) in the logarithmic distribution of the vertical velocity [*Nelson et al*., 2003]. The model is made quasi-3-D by solving vertically averaged shallow water momentum equations coupled with a streamline-based vertical structure and a parameterized secondary flow. FaSTMECH is implemented within the Multi-Dimensional Surface Water Modeling System interface [*McDonald et al*., 2005].

[16] From airborne bathymetric lidar data acquired with the Experimental Advanced Airborne Research Lidar [*McKean et al*., 2009], we defined a channel-centered FaSTMECH flow mesh with 1 m cells for the Bear Valley Creek study reach. We initially assumed a constant $z_o = 0.004$ m and eddy viscosity $= 0.05\ \mathrm{m^2\,s^{-1}}$ and predicted flow characteristics during a low discharge of $0.93\ \mathrm{m^3\,s^{-1}}$. Water surface elevations were measured with a total station survey and velocity distributions were collected with an acoustic Doppler velocimeter at two cross sections. The lateral eddy viscosity was kept constant after a sensitivity analysis produced negligible changes in transverse flow structure and water surface elevation when this parameter was varied by ±50%, similar to the result of *Miller and Cluer* [1998]. The model was then calibrated by adjusting z_o until the best match was achieved between predicted and observed water surface elevations at that flow [*Pasternack et al*., 2006; *Pasternack*, 2011; *Pasternack and Senter*, 2011]. This best fit had a standard error of 0.005 m and a root-mean-square error of 0.03 m and was realized with $z_o = 0.006$ m, which is 15% of the substrate d_{50} for the overall study reach (Figure 5a). This value is smaller than the 0.2 d_{50} reported by *Whiting and Dietrich* [1991] for a gravel bed river, but larger than that suggested by *Clifford et al*. [1992] for grain resistance. The former was measured in the field with resistance generated by streambed irregularities with length scales larger than the grains. The latter was measured at the grain scale in an experiment with a featureless streambed. Our topographical survey and numerical mesh capture the resistance generated by irregularities larger than 1 m but not those smaller than 1 m. Thus, our value of 15% of the d_{50} is within the expected range. When z_o was lowered to 0.005 and 0.004 m, the mean water surface elevation was lower than observed and the root-mean-square error increased to 10% and 15%. Raising z_o to 0.007 and 0.009 m increased the mean water surface error to 0.008 and 0.012 m and the root-mean-square error to 8% and 25%. Changes in z_o away from 0.006 m also decreased the accuracy of the predicted velocity distributions (see Figure 5b for the velocity and depth predictions at two cross sections using $z_o = 0.006$ m and eddy viscosity $= 0.05\ \mathrm{m^2\,s^{-1}}$). Following the calibration, this value of z_o was used in all subsequent simulations. However, as described by (2), even when z_o was constant, flow resistance still varied spatially as a function of water depth.

[17] At discharges larger than bankfull, the inundated floodplain roughness could be higher than that of the streambed. The floodplain vegetation in the study area is tall grass with a few short shrubs and no overhanging vegetation near the top of the banks. These plants are also quite flexible and tend to bend parallel to the flow, reducing their ability to redirect or focus flow toward the main channel. The fine discretization of the flow mesh, allowed by the detailed topobathymetric survey, describes roughness at scales larger than about 1 m, leaving only smaller-scale effects to be represented by model parameters [*Lane and Bates*, 1998; *Lane and Richards*, 2001; *Lane and Ferguson*, 2005; *Morvan et al*., 2008]. To account for the resistance added by floodplain vegetation, we used a z_o of 0.02 m in those areas of the flow mesh, which may generate quite high drag coeffi-

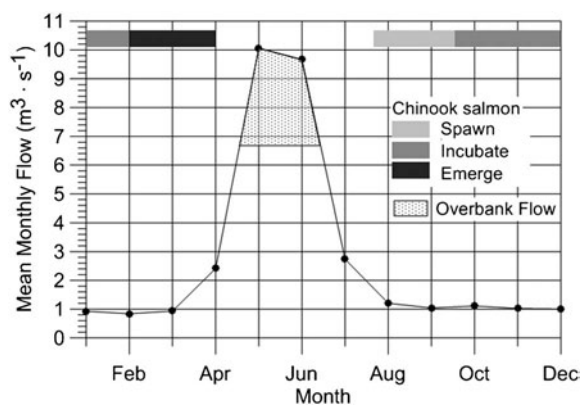

Figure 4. Upper Bear Valley Creek 1929–2010 mean monthly hydrograph with approximate period of overbank flow (shaded area) and local Chinook salmon life stages. Hydrograph is scaled by watershed area from the record at USGS gauge 13309000 in lower Bear Valley Creek.

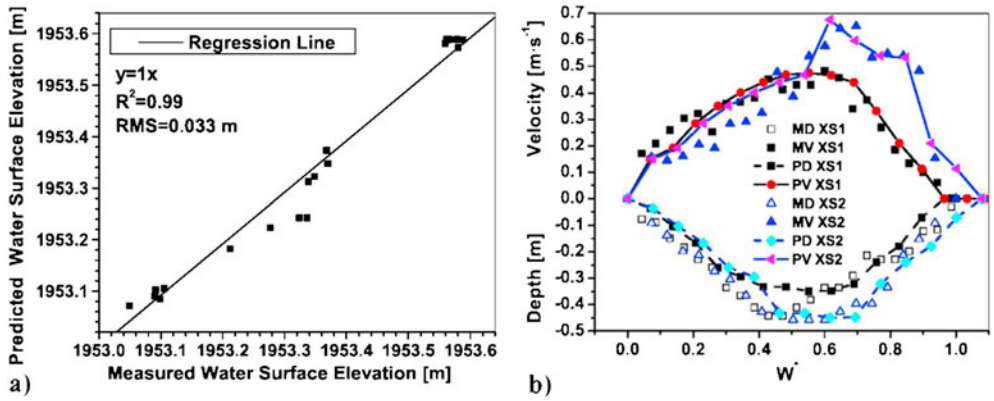

Figure 5. Comparison between model predicted and observed: (a) water surface elevation and (b) depth-averaged mean velocity at the calibration discharge of 0.93 $m^3 s^{-1}$ within a 200 m long calibration reach located near the center of the study area. M, P, D, and V represent measured and predicted depth and velocity, respectively. W^* is the station distance normalized by channel width.

cients due to the low depths in those areas. The calculated Manning's n over the floodplain is about 0.1 $s^{1/3} m^{-1}$.

[18] The model was validated by comparing predicted and measured water surface elevations at a discharge of 1.7 $m^3 s^{-1}$ and depth-averaged water velocities along two cross sections and over a range of discharges between 1 and 6 $m^3 s^{-1}$ (Figures 6a and 6b). The calibrated and validated model was then used to predict flow conditions during discharges ranging from 1 to 27 $m^3 s^{-1}$. The upper limit of model discharges was chosen because it has a recurrence interval of ~10 years based on the discharge record scaled from USGS gauges 13309000 in lower Bear Valley Creek and 13295000 in nearby Valley Creek. The scaling between Valley Creek and Bear Valley Creek was done by comparing the two station records between 1930 and 1960, which allowed definition of monthly scaling factors. The scaling factors have low variability with coefficients of variation less than 0.2. The scaling between the gauge at lower Bear Valley Creek and the study site was based on drainage area ratio. We checked the performance of the scaled values by comparing measured discharges at the study site and scaled values. Errors were below 16% (Table 1), which is comparable to those typical of transect-based discharge measurements. The maximum model flow frequency is beyond the 5–7 year life cycle of Chinook salmon, and therefore, flows of this magnitude may affect one generation of spawning salmon, but are unlikely to influence successive generations, and thus the viability of the fish population [*Tonina et al.*, 2008].

4. Modeled Sediment Mobility

[19] We calculated the local bed mobility by comparing the discharge-dependent near-bed shear stress, τ, predicted by the numerical flow model, with the critical shear stress ($\tau_{c,i}$) for each sediment size (i) found in the study reaches (Figure 3). The size heterogeneity in these alluvial channels reduces the mobility of smaller particles that can be sheltered from the flow by larger grains. In turn, the larger particles are more exposed to the flow as they protrude above the smaller grains, and thus, their mobility is increased relative to what it would be if they were surrounded by similar-sized larger particles in sediment with a uniform grain size. To account for this mixed grain size effect, we first estimated the dimensionless critical shear stress ($\tau^*_{c,i}$) for each grain

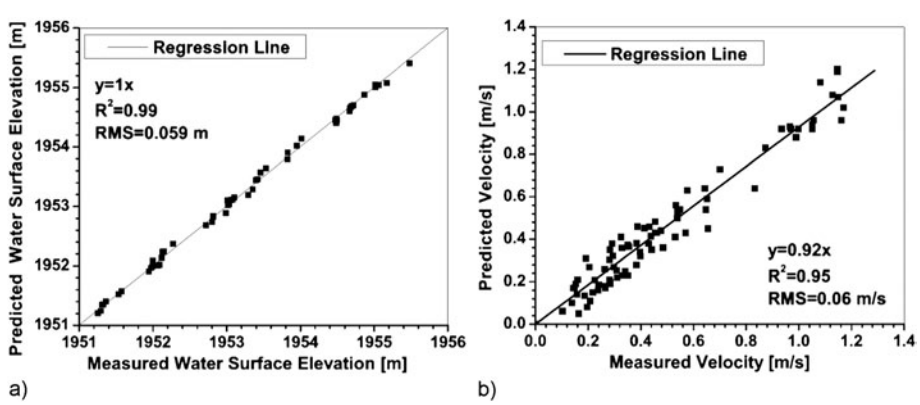

Figure 6. Comparison between model predicted and observed: (a) water surface elevation along the 1.6 km long study site at a discharge of 1.6 $m^3 s^{-1}$ and (b) depth-averaged mean velocity for a range of discharges between 1 and 6 $m^3 s^{-1}$.

Table 1. Comparison Between Discharges Measured at Study Site and Scaled From Gauging Stations[a]

Date	Measured Discharge ($m^3 s^{-1}$)	Scaled Discharge ($m^3 s^{-1}$)	Error (%)
7/25/2006	1.61	1.69	4.80
8/23/2007	0.93	0.78	−16.01
7/1/2008	6.18	6.36	2.91
7/9/2008	3.55	3.64	2.51
7/11/2008	3.32	3.23	−2.74
7/14/2008	2.92	2.65	−9.35
7/17/2008	2.53	2.37	−6.55
7/23/2008	2.95	2.47	−16.40
8/1/2008	1.92	1.67	−12.97
10/2/2008	1.15	0.98	−15.10
10/22/2011	1.58	1.44	−8.37

[a]Dates are formatted as month/day/year.

diameter (d_i) using the method of *Andrews and Parker* [1987] for surface material:

$$\tau^*_{c,i} = \theta_c \left[\frac{d_i}{d_{50}}\right]^m \tag{3}$$

[20] Here d_{50} is the surface grain median diameter for each study reach and θ_c is the critical dimensionless Shields stress of the median grain size on the bed surface. A range of critical shear stresses has been reported in the literature: from small values of 0.03 for loosely packed sediment to high values of 0.06 reported for imbricated particles [*Buffington and Montgomery*, 1997]. We selected $\theta_c = 0.0455$ because: a) visual inspection of the streambed shows imbricated particles, b) bed load measurements at near-bankfull flow revealed low amounts of sand and small gravel transport, suggesting high critical shear stresses, c) the estimated sediment mobility is close to our preliminary field observations presented later in Table 4 at near-bankfull flow and d) this critical stress is in the middle of the range found by *Buffington and Montgomery* [1997]. This value was also suggested in the analysis by *Andrews and Parker* [1987] of data from Oak Creek, Oregon, which is a small gravel bed stream with physical characteristics similar to those in our study area. Previous field and laboratory studies have found the exponent m to commonly vary between −0.65 and −1 and we used $m = -0.9067$, again following the development of a hiding function for surface material from the analysis of Oak Creek data by *Andrews and Parker* [1987].

[21] The critical shear stress for each grain diameter is then

$$\tau_{c,i} = \tau^*_{c,i}\, g\,(\rho_s - \rho_w)\, d_i \tag{4}$$

where $g = 9.8\ \mathrm{m\,s^{-2}}$ and ρ_s and ρ_w are 2650 and 1000 $\mathrm{kg\,m^{-3}}$, respectively (Figure 7).

[22] The computed mobility for each grain size was first used to quantify the percent of streambed area, $A(\tau > \tau_{c,i})_i$, where the ith grain size was expected to be mobile, assuming that the surface particles were all the ith grain size. This prediction was made for the range of study discharges (1 to 27 $\mathrm{m^3\,s^{-1}}$). Then, to account for the mix of grain sizes present, the mobility calculations by individual sizes were convolved with the measured distribution of grain sizes to predict the percent area of the streambed that was mobile (A_e) using

$$A_e = \left[A\left(\tau \geq \tau_{c,p\max}\right)\beta_{p\max} + \sum_{i=1}^{i=p\max-1}\left(A\left(\tau \geq \tau_{c,i}\right) - A\left(\tau \geq \tau_{c,i+1}\right)\right)\beta_i\right]\frac{100}{A_T} \tag{5}$$

where β is the cumulative fractional distribution of grain sizes, $p_{\max}$ is the largest grain size class, and A_T is the total streambed area. This mobility analysis was done for both the overall channel bed in the study reach (using A_T in (5)) and just the salmon spawning areas that have a slightly finer grain size distribution than that of the overall bed (then $A_T = A_{sp} =$ constant). For the calculation of mobility in the overall channel bed, A_T varied with discharge up to bankfull conditions (6.7 $\mathrm{m^3\,s^{-1}}$), but then remained constant for higher flows, during which some of the water spilled outside the main stem channel.

5. Field Measurements

[23] Bed load transport was measured in upper Bear Valley Creek on 1 July 2008. This was just after the peak snowmelt runoff and the local discharge was 6.2 $\mathrm{m^3\,s^{-1}}$ (93% of bankfull). The bed load measurements were made using a Helley-Smith sampler with a 7.62 cm entrance nozzle. Ten samples were taken on a single transect across the channel and the collection time for each sample was 60 s. The 10 samples were then aggregated into one bulk sample, which yielded a transport rate of 0.305 $\mathrm{kg\,h^{-1}}$.

[24] Results of 16 years of ground and aerial surveys of annual Chinook salmon redd construction were used to define spawning areas that were consistently occupied by multiple generations of fish [*Thurow*, 2000]. These areas were generally convexities in the channel bed, although not always at the tail sections of pools as often described in published literature [e.g., *Bjornn and Reiser*, 1991]. This is consistent with a 2005 high-spatial-resolution survey of the locations of 57 salmon redds in the study area. In that year, 29 redds were in the classic position of tail sections of pools (or the upstream face of the next downstream bed convexity), 11 were on the crest of a bed convexity, 15 were on a downstream face of a convexity (or the flow entrance to the next downstream pool), and 1 was on the side of a pool.

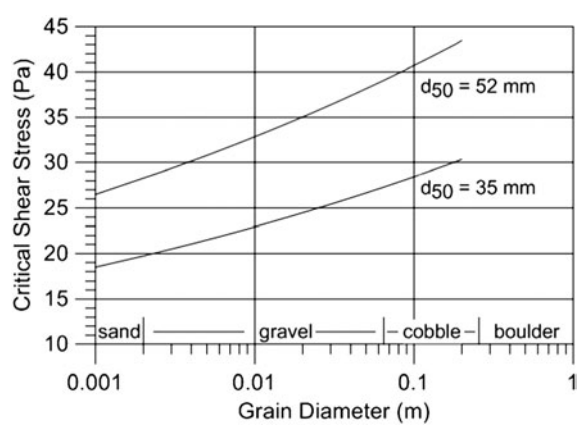

Figure 7. Critical shear stress predicted by (3) and (4) by grain diameter. Particle size classes are indicated above the grain diameter scale.

Table 2. Shields Stresses and Shear Stresses Relative to Critical for d_{50} and Small Gravel

$Q = 6\,m^3\,s^{-1}$			$Q = 10\,m^3\,s^{-1}$		
Median Shields Stress	Area With Shear Stress > $\tau_{c,d_{50}}$ (%)	Area With Shear Stress > $\tau_{c,2mm}$ (%)	Median Shields Stress	Area With Shear Stress > $\tau_{c,d_{50}}$ (%)	Area With Shear Stress > $\tau_{c,2mm}$ (%)
0.005	1.2	2.3	0.005	1.3	2.6

6. Results

6.1. Model Shields Stresses

[25] We report the FaSTMECH simulations of stresses at discharges between 6 and 27 $m^3\,s^{-1}$. Flows of 10 $m^3\,s^{-1}$ (~150% bankfull) are the most frequent overbank discharges in this channel and occur during each snowmelt season, while flows of 17 and 27 $m^3\,s^{-1}$ have recurrence intervals of ~2 and ~10 years, respectively. We first compare stress patterns during discharges of 6 and 10 $m^3\,s^{-1}$. Shear stresses were generally low during both flow conditions (Table 2). The median Shields stresses did not change as flows increased from near bankfull to overbank. The portion of the model domain in which near-bed shear stresses were larger than critical, for either the d_{50} particle size or the smallest gravel size (2 mm), also increased very little during the higher flow.

[26] The spatial patterns of Shields stresses are shown in Figure 8 and the highest stresses were in a central core of flow in each stream with lower stresses on the margins of flow. As discharge grew from 6 to10 $m^3\,s^{-1}$, these central flow cores expanded in area, while the maximum stresses within those zones only slightly increased (see histogram in Figure 8).

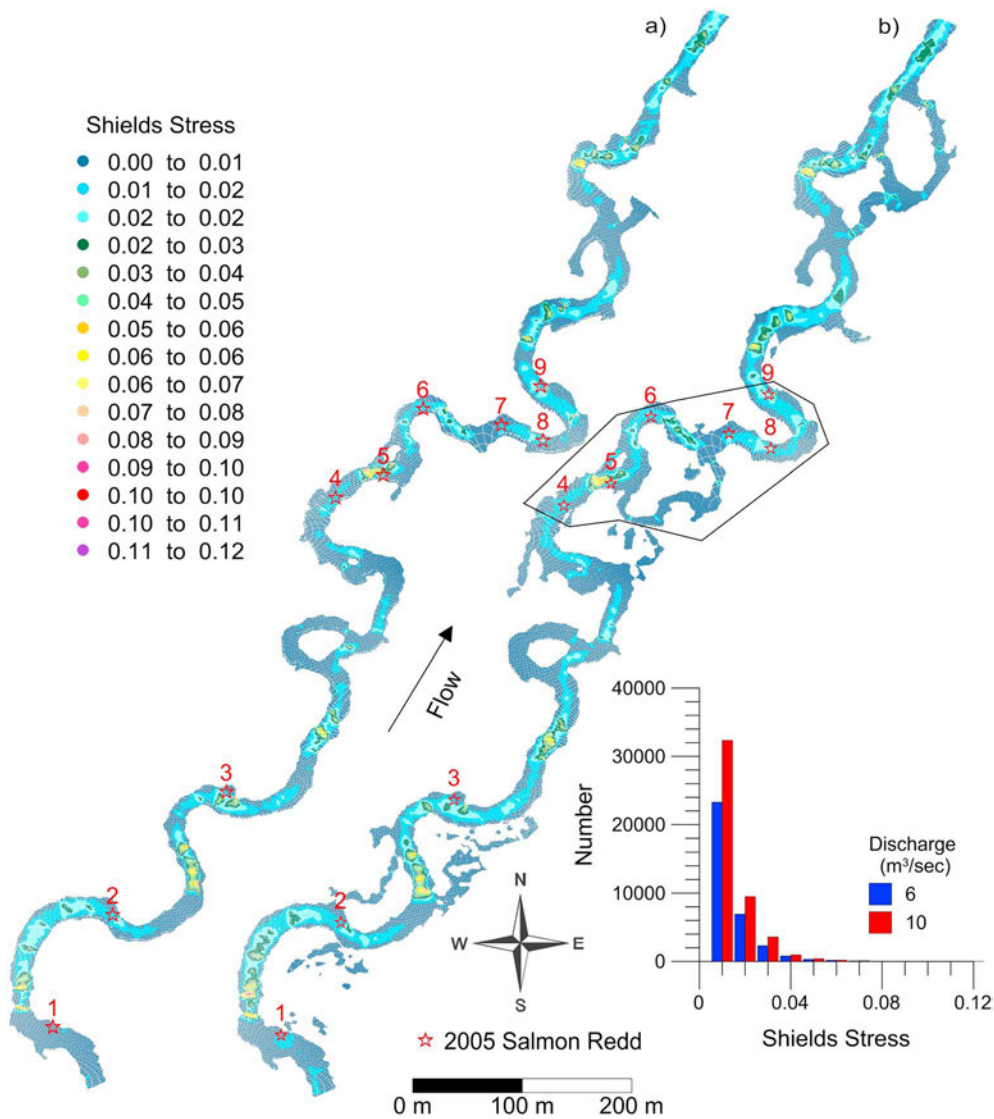

Figure 8. Shields stresses calculated for $d_{50} = 52$ mm: (a) $Q = 6\,m^3\,s^{-1}$, (b) $Q = 10\,m^3\,s^{-1}$. The 2005 salmon redd numbers correspond to those in Figure 11. The area in black polygon in Figure 8b is shown in detail in Figure 9.

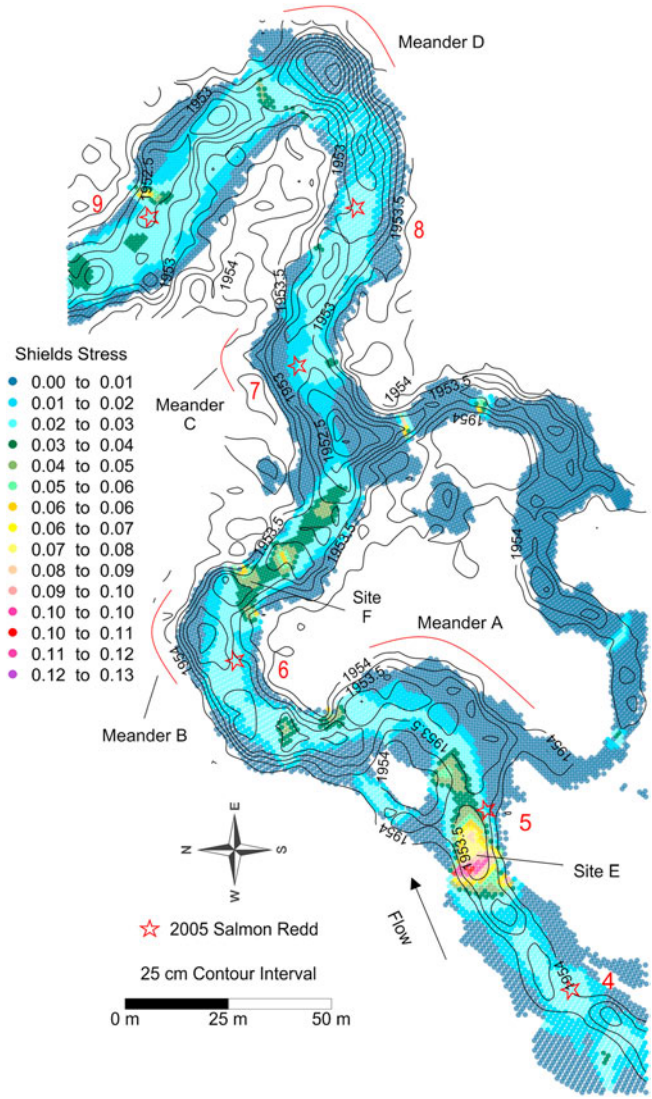

Figure 9. Enlarged view of Shields stresses and bed topography during an overbank discharge of $10\,m^3\,s^{-1}$. Shields stresses were calculated for spawning areas with $d_{50} = 35$ mm. The 2005 salmon redd numbers (in red) correspond to those in Figures 8 and 11 and the symbol size approximately encompasses each redd. See Figure 8 for reach location.

The greatest effects of the higher discharge were flows spreading out, widening of the marginal areas of low shear stress, and in some locations flows moved into semiabandoned channels adjacent to the modern main stem, where again the shear stresses were very low (Figure 8).

[27] Figure 9 shows an enlarged view and the details of the pattern of Shields stresses at a discharge of $10\,m^3\,s^{-1}$ in a 350 m long reach of Bear Valley Creek (see Figure 8b for the location of this reach). At this stage, the flow expanded into the old meander bend on the right side of the channel where small Shields stresses developed in the low-velocity water. In the main channel, the marginal areas of low stress were nearly continuous on both sides of the channel. The central flow core with higher stresses tended to cross the depositional bars on the inside of meander bends and bypass the deeper water and pools on the outside of the meanders (see examples at Meanders A–D, Figure 9). The highest Shields

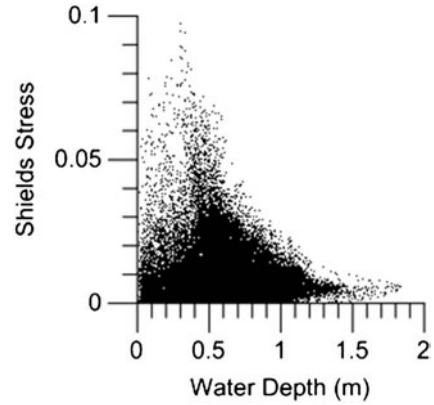

Figure 10. Modeled near-bed Shields stresses as a function of water depth during a discharge of $10\,m^3\,s^{-1}$.

stresses in the reach occurred where the bed morphology forced the depth of the central core of flow to decrease, while the flow remained laterally confined (Site E). A lateral constriction in the channel at Site F also caused higher stresses.

[28] As suggested by their spatial distributions, Shields stresses varied with flow depth and, at a discharge of $10\,m^3\,s^{-1}$, the largest stresses were in depths of 40–60 cm (Figure 10). Stresses declined sharply in depths less than about 10 cm and greater than about 70 cm.

[29] In 2005, nine redds were constructed by spawning Chinook salmon in the Bear Valley study reach. These spawning sites were identified in the field and the locations of the egg deposits were surveyed with a spatial accuracy of ±1 m (see Figures 8 and 9 for locations). Modeled Shields stresses at these redd sites during three overbank flow conditions were averaged over a $2\,m^2$ area, typical of the size of local salmon egg pockets. The Shields stresses at the redd sites were below 0.035 at flows up to $17\,m^3\,s^{-1}$ and only one site experienced stress >0.05 even during a simulated 10 year

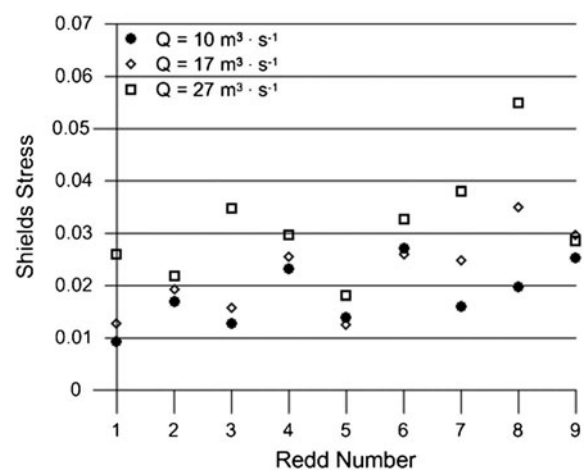

Figure 11. Modeled dimensionless Shields stress at surveyed redd sites using $d_{50} = 35$ mm. Dimensionless Shields stresses of about 0.03 are commonly considered about the lower limit for incipient motion of particles on a mixed-size gravel bed, and values >0.06 or 0.07 correspond to full bed mobility [e.g., *Buffington and Montgomery*, 1997; *Lisle et al.*, 2000]. The locations of numbered redds are shown in Figures 8 and 9.

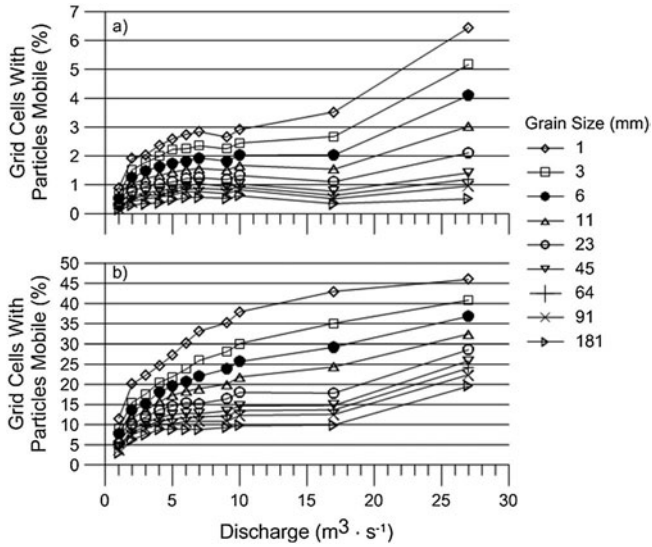

Figure 12. Percent of channel bed surface area predicted to be mobile as a function of particle diameter and discharge. (a) Whole model domain ($d_{50} = 52$ mm). (b) Spawning areas only ($d_{50} = 35$ mm).

event (Figure 11). Redds tended to be constructed off the center of flow, thus avoiding the highest velocities and shear stresses as noted by *Quinn* [2005] (see Figures 8 and 9 and in particular Redd 5 on the margin of a high-stress area).

6.2. Substrate and Bed Mobility Patterns

[30] The predicted mobility of substrate materials by grain size and discharge is shown in Figures 12a and 12b for the entire channel bed and just the spawning areas, respectively. These mobility curves were computed by comparing the near-bed shear stress at a given discharge at each flow mesh node with the size-dependent critical stress defined by (4). They can be interpreted as the percent area in which each single grain size (d_i) would be expected to be mobile. At all discharges, the mobile area consistently increased with smaller particle sizes, despite the shielding effects for mixed grains (3). For all grain sizes, the mobility of the whole bed increased steadily during flows from 1 to 7 $m^3 s^{-1}$ (Figure 12a). Then as overbank flows grew from 7 to 17 $m^3 s^{-1}$, grain mobility remained relatively constant except for particles smaller than 3 mm whose mobility slightly increased. At the highest flow, grain mobility increased again

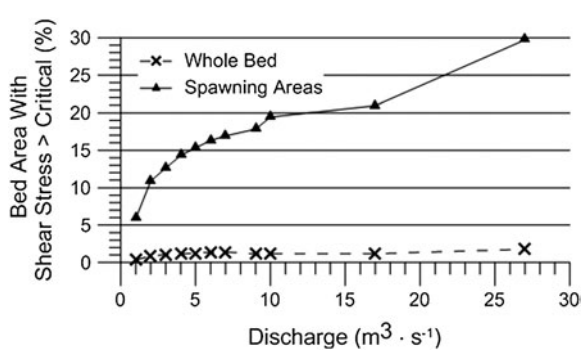

Figure 13. Percent of channel bed surface area predicted to be mobile as a function of discharge.

Table 3. Measured Bed Load Transport by Particle Size at 93% of Bankfull Flow

	Weight (g (%))	Flux (kg/h)
Gravel (>2 mm)	17.77 (35)	0.107
Sand (<2 mm)	33.03 (65)	0.198
Total	50.80	0.305

with the largest effect in grains smaller than 23 mm. During this extreme discharge, in some places, water was confined by the impermeable lateral boundaries of the flow mesh which were about 100 m beyond the channel banks. This may have enhanced the main channel grain mobility, although we have not formally tested for this effect.

[31] For all grain sizes, the percent of spawning areas predicted to be mobile was greater at each discharge (Figure 12b), relative to overall channel conditions. This is a combined effect of consistently higher near-bed shear stresses in the spawning areas and lower critical stresses resulting from the smaller d_{50} in those sites. As flows increased from 9 to 17 $m^3 s^{-1}$ and went outside the channel banks, the mobility of grains larger than 11 mm remained essentially constant, while smaller-sized sediment mobility increased. At the highest flow, the mobility of all grain sizes again increased. The range of substrate sizes preferred for spawning by Chinook salmon includes gravel-sized sediment with particle diameters ranging from 16 to 128 mm [*Bjornn and Reiser*, 1991; *Kondolf and Wolman*, 1993; *Quinn*, 2005]. At bankfull flows (6.7 $m^3 s^{-1}$) in Bear Valley Creek, about 0.5–1.5% of the overall streambed area and 10–17% of the surface area of spawning sites had shear stresses large enough to mobilize particles within this size range (Figures 12a and 12b). These areas of potential gravel mobility are concentrated in the central core of the flow and particularly where the flow shoaled and converged. For flows to entirely scour a salmon redd, even the largest particles in the streambed would have to be mobile. At bankfull flows, all sediment sizes are mobile in only 10% of the spawning area, as illustrated by the curve for mobility of the largest particle with a diameter of 181 mm in Figure 12b. During the most extreme 10 year event, this percentage rises to 19% of spawning areas. Using the same criterion, only about 0.5% of the entire streambed area has complete grain mobility during any of the modeled discharges (Figure 12a).

[32] Figure 13 shows the predicted mobility of the channel beds after the convolutions of particle size-dependent mobility with the actual grain size distributions. At bankfull flows, about 2% of the total area of the model reach was mobile and the percentage of mobility remained low during overbank flows. In the bankfull flow condition, 17% of the surfaces of the spawning areas were mobile. This result was consistent with the shear stress predictions at actual redd sites, which were below the critical values for mobility of particles in the size range commonly

Table 4. Predicted and Observed Maximum Mobile Grain Diameters

Maximum Model Shear Stress (Pa)	d_{max} Predicted Mobile[a] (mm)	d_{max} Sampled (mm)
22	6	4–6

[a]Predicted using the $d_{50} = 35$ mm curve in Figure 7.

used by spawning Chinook salmon (Figure 11). As flows grew beyond bankfull, the mobility of the spawning areas increased slightly to 21% at a discharge of $17\,m^3\,s^{-1}$ before rising to 30% in the most extreme flow condition.

6.3. Field Bed Load Transport Measurements

[33] The field bed load transport measurement made at about 93% of bankfull flow was generally consistent with the results of the numerical flow and bed mobility analyses. The total transport rate was quite low ($0.305\,kg\,h^{-1}$) and dominated by sand movement (Table 3 and Figure 3). We used the bed load transport measurements to perform a simple validation test of the numerical flow model. The largest grain size sampled at the cross section during a flow of $6.3\,m^3\,s^{-1}$ was compared with the model prediction of the largest mobile grain diameter using (4) (Figure 7) and the $6\,m^3\,s^{-1}$ model discharge. The predicted maximum grain size closely matched that of the observed (Table 4).

7. Discussion

[34] Our finding of low shear stresses and little bed mobility, even at flows much greater than bankfull, is inconsistent with the traditional view of general bed mobility developing at near-bankfull conditions. However, many field, laboratory, and numerical studies have documented and predicted less than full bed mobility during flows at or even above bankfull. For example, *Andrews and Erman* [1986] studied patterns of bed load transport during a snowmelt runoff period in Sagehen Creek, a small high-elevation California mountain stream with characteristics similar to those in the upper MFSR tributaries. During the snowmelt period, Sagehen Creek experienced flows that were approximately twice that of bankfull, but in this unconfined channel, the reach-averaged dimensionless shear stress never exceeded about 125% of the critical value. Furthermore, the bed load transport rate was small and an armor layer of coarser grains persisted through the snowmelt event, despite the transport of particles with nearly all available sizes, including those much larger than the median size on the bed surface [*Andrews and Erman*, 1986]. This style of intermittent exchange of a few particles in an otherwise intact armor layer led *Parker et al.* [1982] to name this condition "pavement" or "mobile armor." Persistence of a mobile armor layer during periods of bed load transport has also been documented in a variety of other flume and field settings [e.g., *Parker and Klingeman*, 1982; *Andrews and Parker*, 1987; *Carling*, 1988; *Wilcock and McArdell*, 1997; *Wilcock and DeTemple*, 2005; *Clayton and Pitlick*, 2007]. *Hassan et al.* [2006] noted that flat hydrographs, of the style produced by snowmelt in mountain streams like Bear Valley Creek, favor the formation of armored bed surfaces. It is also commonly observed in armored systems that the transported load is much finer than the bed surface sediment, as we see in Figure 3.

[35] *Lisle et al.* [2000] also observed limited bed mobility in cases of sediment-poor gravel bed channels and found that during bankfull conditions, the majority of the bed load was derived from small areas of high transport. As previously noted, they used categories of $\tau^* < 0.03$, $0.03 < \tau^* < 0.06$, and $\tau^* > 0.06$ to define immobile, partially mobile, and fully mobile bed surfaces, respectively. In Jacoby Creek, *Lisle et al.* [2000] reported that about 35% of the bed surface was immobile, 46% partially mobile, and only 19% fully mobile during bankfull flows. The bankfull discharge and gradient in Jacoby Creek are about twice those of our study stream, while the bankfull channel width is 80% of that in Bear Valley, and the d_{50} is 36 mm; thus, the conditions in Jacoby Creek are conducive to higher bed stresses and greater mobility than those in our study area. Using these same τ^* mobility classes, during bankfull flows in Bear Valley Creek, we predict that about 96% of the streambed is immobile, 3.5% is partially mobile, and 0.5% is fully mobile. In their numerical and field study of a regulated river, *May et al.* [2009] used mobility classes calibrated by tracer rock and scour chain observations and reported that during a flood that was 111% of bankfull discharge, only 18% of their study streambed was in a fully mobile condition, 31% of the bed was immobile, and the remaining 51% was partially mobile. *Lisle et al.* [2000] and *May et al.* [2009] both observed that meandering channels force strong spatial variations in near-bed shear stress with stress and mobility concentrated in the central flow core. This is similar to our model predictions of stress patterns in upper Bear Valley (Figures 8 and 9).

[36] The histogram of the predicted Shields number during flows of 6 and $10\,m^3\,s^{-1}$ shows that Shields stresses are predominantly below 0.03 (Figure 8). This suggests that uncertainty related to the selection of a critical Shields number between 0.03 and 0.06 will be very small. It also increases our confidence about predicted particle mobility as it is unlikely that uncertainty in either predicted Shields stresses or critical stresses would strongly affect our results and conclusions.

[37] *Lorang and Hauer* [2003] analyzed reach-averaged conditions at initial motion for 33 sites in gravel bed rivers and found that in 85% of the cases shear stresses had to be as much as 2 times those at bankfull to cause general bed mobility. From observations of an extensive array of tracer particles, *Haschenburger and Wilcock* [2003] found 20–50% of a gravel bed in a condition of partial mobility during a flow that was 85% of bankfull. *Church and Hassan* [2002] also documented movement of only 30% of tracer particles during a 2+ year flood in a gravel bed stream.

[38] Our predictions that near-bed stresses and substrate mobility do not increase significantly when flows exceed bankfull are explained by the geomorphic setting. The floodplains and surrounding low-lying meadows adjacent to Bear Valley and many other MFSR tributaries contain numerous abandoned channel meanders, sloughs, and other low-lying areas whose elevations are near those of the local channel bed. In such a fluvial environment, it is often observed that during the initial phase of overbank flooding, the main stem water level and velocity will not rise and the median depths and velocities may even drop temporarily, until these low-lying areas are filled [e.g., *Nicholas and Mitchell*, 2003; *Andrews and Erman*, 1986]. Our results suggest that the effects of the lack of confinement can persist beyond this transient period and act as a "stress relief valve" during steady state overbank flows in which maximum shear stresses increase little beyond those developed at bankfull. The biological imperative of Chinook salmon to spawn on convexities in the beds of low-gradient gravel bed streams and their dramatic natal fidelity when selecting spawning locations leads populations to concentrate their reproduction in meandering pool-riffle streams. This, in turn, favors unconfined valley settings with maximum shear stresses

limited more by channel and floodplain topography than by the hydrologic regime.

[39] Furthermore, irrespective of channel confinement, peak flows in snowmelt-dominated systems typically have low variability, relative to the mean annual flood. For example, *Pitlick* [1994], in a study of flood frequency curves from several regions in the western U.S., found that in an alpine snowmelt-dominated system, the 100 year flood was less than 2 times the mean annual flood, while the ratio in coastal drainages was 3 to 6 times and in semiarid systems up to 10 times the mean annual flood.

[40] Our analysis of the risk of scour at spawning sites is also probably conservative. Chinook salmon bury their eggs to depths of about 15–50 cm below the streambed surface, although there can be considerable local variability related to, for example, female body size and the details of substrate characteristics [*DeVries*, 1997; *Quinn*, 2005]. Given the limited mobility of the surface of the channel bed in Bear Valley Creek, it is even more unlikely that scour will occur to the depths of egg burial. This observation is consistent with the results of *Lapointe et al*. [2000] who used reach-averaged shear and critical shear stress calculations to predict a mobility index for different reaches in the Sainte-Marguerite River, Quebec, Canada. Observations of scour depths in that river, relative to Atlantic salmon egg burial depths, showed that in frequent smaller floods there was only a 5% probability of redd scour and even in large floods with a return interval of several centuries the likelihood only rose to about 20% [*Lapointe et al*., 2000].

[41] Our field observations and model predictions indicate that valley and stream morphology, rather than hydrology, control the maximum shear stresses and bed mobility. Consequently, in this context, the details of the hydrologic regime in future climates are less significant and we predict relatively limited channel bed mobility and scour regardless of slightly higher or earlier peak snowmelt runoff, or rain-on-snow or rain events. We also expect that our results will be robust even if the sediment supply would vary due to climate change. Various future climate scenarios forecast higher air temperatures, smaller snowpacks, and earlier snowmelt in some western U.S. mountain watersheds [e.g., *Hayhoe et al*., 2004; *Stewart et al*., 2004, 2005; *Stewart*, 2009; *Pederson et al*., 2011]. These conditions may increase wildfire frequency and severity [*Westerling et al*., 2006; *Morgan et al*., 2008; *Littell et al*., 2009] and in turn trigger greater hillslope erosion. However, unconfined channels in this and similar watersheds are largely disconnected from the surrounding slopes, and it is difficult to deliver eroded sediment across the broad floodplains and into the channels. If more sediment did reach the channels, this increased supply would be unlikely to enhance the gravel bed mobility because, while the developed shear stresses will mobilize fine material (<2 mm), they are insufficient to move gravel-sized particles.

[42] Although we predict and observe little gravel transport in Bear Valley Creek, it is, however, a gravel bed stream and we interpret this substrate condition as primarily a glacial legacy. Debris from the Bull Lake- and Pinedale-age glaciers filled the valley with a mix of sediment from the granitic source area [*Schmidt and Mackin*, 1970]. Glacial activity declined markedly about 15,000 years before present, and since that time, the stream has moved lightly across the glaciofluvial deposits, only slightly lowering the surface of the valley. The modern stream is capable of moving mostly sand and silt through the channel system during the annual snowmelt runoff and this activity winnows the bed, leaving a gravel surface armor. The stream has also migrated laterally, as evidenced by numerous abandoned meanders in the meadow surface, although the ages of these older channel positions are unknown and some of them may be late Pinedale-age features. Field observations suggest that much of the limited gravel transport is the local redistribution of coarse particles input into the channel by nearby bank scour during lateral migrations.

[43] Whereas we use a conventional force balance analysis of substrate motion, our multidimensional numerical hydrodynamics model offers several advantages over reach-averaged calculations or 1-D numerical predictions of shear stress. It is possible in multidimensional models to simulate channel conditions with a meter-scale spatial resolution that matches the scale of microhabitats important to spawning salmon [*Leclerc et al*., 1995]. A multidimensional model also more accurately describes the local hydraulics and shear stress patterns in channels with the pool-riffle morphology preferred for spawning [*Brown and Pasternack*, 2009]. However, multidimensional models can be sensitive to errors in the flow-bounding DEM [e.g., *Ghanem et al*., 1996; *Leclerc et al*., 1995; *Pasternack et al*., 2011], and previously it was not logistically possible to adequately define the model boundary conditions over stream lengths beyond a few hundred meters. Recent innovations in remote sensing of streams have begun to overcome this problem [e.g., *McKean et al*., 2006; *Marcus and Fonstad*, 2008; *Legleiter et al*., 2009; *McKean et al*., 2009], and multidimensional models can be run at kilometric scales with the domain limitation imposed more by the computational burden [*Tonina and McKean*, 2010; *Tonina et al*., 2011].

8. Conclusions

[44] Chinook salmon strongly favor convexities in the beds of gravel bed streams as spawning habitat. In wood-poor streams, this dictates that the fish are most successful by spawning in meandering reaches where the local hydraulics forces this morphology. In postglacial landscapes, such as the tributaries of the MFSR, these meandering stream segments are concentrated in wide and gently sloping valleys. This investigation tests the potential for mobility of the gravel beds of unconfined streams in low-gradient meadows during high discharges ranging up to 300% of bankfull and having a recurrence interval of up to about 10 years. In our study area, we predict mobility of ~2% of the overall surface of the channel bed and ≤20% of the surface of historic spawning areas during 2 year flows which are frequent enough to possibly permanently reduce the reproductive viability of the salmon population. Field measurements of low bed load transport during near-bankfull flows support the model simulations.

[45] The mountain streams of the MFSR that host the majority of Chinook salmon spawning annually experience overbank flooding during the spring-early summer snowmelt. But the combination of low stream gradient, low sediment supply, and the stress relief valve of the unconfined meadows causes relatively static stream morphology in all flow conditions, including overbank flows. The maximum shear stresses

are established more by the unconfined morphology than the stream discharge. Thus, although it is possible that future hydrologic regimes in these streams may include smaller (or larger) snowpacks, earlier snowmelt runoff peaks that occur during the salmon incubation period, and increased likelihood of rain-on-snow or rain events, there is limited vulnerability of autumn-spawning Chinook salmon in the MFSR, and similar landscapes, to the risk of extensive streambed mobility and substrate scour that could destroy salmon egg nests. The geomorphic setting of their natal streams largely protects these fish from this dimension of climate variability and change.

[46] **Acknowledgments.** Wayne Wright, Virgil Rabine, and Richard Mitchell expertly acquired the bathymetric lidar data. Dan Isaak assisted with the 2005 field survey of Chinook salmon redds, and Russ Thurow kindly provided data from the 2009 MFSR salmon spawning aerial survey. The manuscript was significantly improved by the helpful comments of John Pitlick (Associate Editor), Peter Wilcock, Tom Lisle, Rich McDonald, and an anonymous reviewer. We are grateful to the U.S. Forest Service, Rocky Mountain Research Station for project financial support.

References

Andrews, E. D. (1983), Entrainment of gravel from naturally sorted riverbed material, *Geol. Soc. Am. Bull.*, *94*, 1225–1231.

Andrews, E. D. (1984), Bed-material entrainment and hydraulic geometry of gravel-bed rivers in Colorado, *Geol. Soc. Am. Bull.*, *95*, 371–378.

Andrews, E. D., and D. C. Erman (1986), Persistence in the size distribution of surficial bed material during an extreme snowmelt flood, *Water Resour. Res.*, *22*, 191–197.

Andrews, J., and L. B. Everson (1988), Middle Fork and Upper Salmon River Habitat Improvement Implementation Plan: FY 1988–1992, *Proj. 84-24, DE-AI79-84BP17579*, 36 pp., Div. of Fish and Wildl., Bonneville Power Admin., Portland, Oreg.

Andrews, E. D., and G. Parker (1987), Formation of a coarse surface layer as the response to gravel mobility, in *Sediment Transport in Gravel-Bed Rivers*, edited by C. R. Thorne et al., pp. 269–300, John Wiley, Chichester, U. K.

Bales, R. C., N. P. Molotch, T. H. Painter, M. D. Dettinger, R. Rice, and J. Dozier (2006), Mountain hydrology in the western United States, *Water Resour. Res.*, *42*, W08432, doi:10.1029/2005WR004387.

Battin, J., M. W. Wiley, M. H. Ruckelshaus, R. N. Palmer, E. Korb, K. K. Bartz, and H. Imaki (2007), Projected impacts of climate change on salmon habitat restoration, *Proc. Natl. Acad. Sci. U. S. A.*, *104*, 6720–6725.

Beebee, R. A., and M. Manga (2004), Variation in the relationship between snowmelt runoff in Oregon and ENSO and PDO, *J. Am. Water Resour. Assoc.*, *40*, 1011–1024.

Beniston, M., F. Keller, and S. Goyette (2003), Snow pack in the Swiss Alps under changing climatic conditions: An empirical approach for climate impacts studies, *Theor. Appl. Climatol.*, *74*, 19–31.

Bjornn, T. C., and D. W. Reiser (1991), Habitat requirements of salmonids in stream, in *Influences of Forest and Rangeland Management on Salmonid Fishes and Their Habitats*, *Spec. Publ. 19*, edited by W. R. Meehan, pp. 83–138, Am. Fish. Soc., Bethesda, Md.

Brown, R. A., and G. B. Pasternack (2009), Comparison of methods for analyzing salmon habitat rehabilitation designs for regulated rivers, *River Res. Appl.*, *25*, 745–772.

Buffington, J. M., and D. R. Montgomery (1997), A systematic analysis of eight decades of incipient motion studies, with special reference to gravel-bedded rivers, *Water Resour. Res.*, *33*(8), 1993–2029.

Burner, C. J. (1951), Characteristics of spawning nests of Columbia River salmon, *Fish. Bull.*, *52*, 97–110.

Carling, P. (1988), The concept of dominant discharge applied to two gravel-bed streams in relation to channel stability thresholds, *Earth Surface Processes Landforms*, *13*, 355–367.

Church, M., and M. A. Hassan (2002), Mobility of bed material in Harris Creek, *Water Resour. Res.*, *38*(11), 1237, doi:10.1029/2001WR000753.

Clark, M. E., K. A. Rose, D. A. Levine, and W. W. Hargrove (2001), Predicting climate change effects on Appalachian trout: Combining GIS and individual-based modeling, *Ecol. Appl.*, *11*, 161–178.

Clayton, J. A., and J. Pitlick (2007), Persistence of the surface texture of a gravel-bed river during a large flood, *Earth Surf. Processes Landforms*, *33*, 661–673.

Clifford, N. J., A. Robert, and K. S. Richards (1992), Estimation of flow resistance in gravel-bedded rivers: A physical explanation of the multiplier of roughness length, *Earth Surf. Processes Landforms*, *17*(2), 111–126.

Dettinger, M. D., and D. R. Cayan (1995), Large-scale atmospheric forcing of recent trends toward early snowmelt runoff in California, *J. Clim.*, *8*, 606–623.

DeVries, P. (1997), Riverine salmonid egg burial depths: Review of published data and implications for scour studies, *Can. J. Fish. Aquat. Sci.*, *54*, 1685–1698.

Emmett, W. W. (1975), The channels and waters of the upper Salmon River area, Idaho, in *U.S. Geol. Surv. Prof. Pap. 870-A*, 116 pp.

Fisher, F. S., D. H. McIntyre, and K. M. Johnson (1992), Geologic map of the Challis 1°x2° quadrangle, Idaho, *U.S. Geol. Surv. Geol. Invest. Ser. I-1819*.

Gasith, A., and V. H. Resh (1999), Streams in Mediterranean climate regions: Abiotic influences and biotic responses to predictable seasonal events, *Annu. Rev. Ecol. Syst.*, *30*, 51–81.

Ghanem, A., P. Steffler, and F. Hicks (1996), Two-dimensional hydraulic simulation of physical habitat conditions in flowing streams, *Regulated Rivers Res. Manage.*, *12*, 185–200.

Hamlet, A. F., P. W. Mote, M. P. Clark, and D. P. Lettenmaier (2005), Effects of temperature and precipitation variability on snowpack trends in the western United States, *J. Clim.*, *18*, 4545–4561.

Harpold, A., P. Brooks, S. Rajagopal, I. Heidbuchel, A. Jardine, and C. Stielstra (2012), Changes in snowpack accumulation and ablation in the intermountain west, *Water Resour. Res.*, *48*, W11501, doi:10.1029/2012WR011949.

Haschenburger, J. K., and P. R. Wilcock (2003), Partial transport in a natural gravel bed channel, *Water Resour. Res.*, *39*(1), 1020, doi:10.1029/2002WR001532.

Hassan, M. A., R. Egozi, and G. Parker (2006), Experiments on the effect of hydrograph characteristics on vertical grain sorting in gravel bed rivers, *Water Resour. Res.*, *42*, W09408, doi:10.1029/2005WR004707.

Hauer, F. R., J. S. Baron, D. H. Campbell, K. D. Fausch, S. W. Hostetler, G. H. Leavesley, P. R. Leavitt, D. M. McKnight, and J. A. Stanford (1997), Assessment of climate change and freshwater ecosystems of the Rocky Mountains, USA and Canada, *Hydrol. Processes*, *11*, 903–924.

Hayhoe, K., et al. (2004), Emissions pathways, climate change, and impacts on California, *Proc. Natl. Acad. Sci. U. S. A.*, *101*(34), 12,422–12,427.

Holtby, L. B., and M. C. Healy (1986), Selection for adult size in female coho salmon (*Oncorhynchus kisutch*), *Can. J. Fish. Aquat. Sci.*, *43*, 1946–1959.

Isaak, D. J., and R. F. Thurow (2006), Network-scale spatial and temporal variation in Chinook salmon (*Oncorhynchus tshawytscha*) redd distributions: Patterns inferred from spatially continuous replicate surveys, *Can. J. Fish. Aquat. Sci.*, *63*, 285–296.

Jackson, W. L., and R. L. Beschta (1982), A model of two-phase bedload transport in an Oregon Coast Range stream, *Earth Surf. Processes Landforms*, *7*, 517–527.

Jarrett, R. D. (1990), Hydrologic and hydraulic research in mountain rivers, *Water Resour. Bull.*, *26*, 419–429.

King, J. G., W. W. Emmett, P. J. Whiting, R. P. Kenworthy, and J. J. Barry (2004), Sediment transport data and related information for selected coarse-bed streams and rivers in Idaho, *Gen. Tech. Rep. RMRS-GTR-131*, 26 pp., Rocky Mountain Res. Stn., U.S. Dep. of Agric. For. Serv., Fort Collins, Colo.

Kondolf, G. M., and M. G. Wolman (1993), The sizes of salmonid spawning gravels, *Water Resour. Res.*, *29*, 2275–2285.

Kondolf, G. M., G. F. Cada, M. J. Sale, and T. Felando (1991), Distribution and stability of potential salmonid spawning gravels in steep boulder-bed streams of the Eastern Sierra Nevada, *Trans. Am. Fish. Soc.*, *120*, 177–186.

Lane, S. N., and P. D. Bates (1998), Special issue: High resolution flow modelling, *Hydrol. Processes*, *12*(8), 1129–1396.

Lane, S. N., and R. I. Ferguson (2005), Modelling reach-scale fluvial flows, in *Computational Fluid Dynamics: Applications in Environmental Hydraulics*, edited by P. D. Bates et al., pp. 217–269, John Wiley, Chichester, U. K.

Lane, S. N., and K. S. Richards (2001), The "validation" of hydrodynamic models: Some critical perspectives, in *Model Validation for Hydrological and Hydraulic Research*, edited by P. D. Bates and M. G. Anderson, pp. 413–438, John Wiley, Chichester, U. K.

Lapointe, M., B. Eaton, S. Driscoll, and C. Latulippe (2000), Modelling the probability of salmonid egg pocket scour due to floods, *Can. J. Fish. Aquat. Sci.*, *57*, 1120–1130.

Leclerc, M., A. Boudreault, J. Bechara, and G. Corfa (1995), Two-dimensional hydrodynamic modeling: A neglected tool in the instream flow incremental methodology, *Trans. Am. Fish. Soc.*, *124*(5), 645–662.

Legleiter, C. J., D. A. Roberts, and R. L. Lawrence (2009), Spectrally based remote sensing of river bathymetry, *Earth Surf. Processes Landforms*, *34*, 1039–1059.

Lettenmaier, D. P., and T. Y. Gan (1990), Hydrologic sensitivities of the Sacramento-San Joaquin River Basin, California, to global warming, *Water Resour. Res.*, *26*, 69–86.

Li, R.-M., D. B. Simons, and M. A. Stevens (1976), Morphology of cobble-bed streams in small watersheds, *J. Hydraul. Div. Am. Soc. Civ. Eng.*, *102*, 1101–1117.

Lisle, T. (1989), Sediment transport and resulting deposition in spawning gravels, north coastal California, *Water Resour. Res.*, *25*, 1303–1319.

Lisle, T., J. M. Nelson, J. Pitlick, M. Madej, and B. L. Barkett (2000), Variability of bed mobility in natural, gravel-bed channels and adjustments to sediment load at local and reach scales, *Water Resour. Res.*, *36*, 3743–3755.

Littell, J. S., D. McKenzie, D. L. Peterson, and A. L. Westerling (2009), Climate and wildfire area burned in western U.S. ecoprovinces, 1916–2003, *Ecol. Appl.*, *19*, 1003–1021.

Lorang, M. S., and F. R. Hauer (2003), Flow competence and streambed stability: An evaluation of technique and application, *J. N. Am. Benthol. Soc.*, *22*, 475–491.

Marcus, W. A., and M. A. Fonstad (2008), Optical remote mapping of rivers at sub-meter resolutions and watershed extents, *Earth Surf. Processes Landforms*, *33*, 4–24.

Maurer, E. P., I. T. Stewart, C. Bonfils, P. B. Duffy, and D. Cayan (2007), Detection, attribution, and sensitivity of trends toward earlier streamflow in the Sierra Nevada, *J. Geophys. Res.*, *112*, D11118, doi:10.1029/2006JD008088.

May, C. L., B. Pryor, T. E. Lisle, and M. Lang (2009), Coupling hydrodynamic modeling and empirical measures of bed mobility to predict the risk of scour and fill of salmon redds in a large regulated river, *Water Resour. Res.*, *45*, W05402, doi:10.1029/2007WR006498.

McDonald, R. R., J. M. Nelson, and J. P. Bennett (2005), Multi-dimensional surface-water modeling system user's guide, online documentation, U.S. Geol. Surv., Golden, Colo., [Available at http://wwwbrr.cr.usgs.gov/projects/GEOMORPH_Lab/WebHelp_Pro/MD_SWMS.htm.]

McKean, J., C. W. Wright, P. Kinzel, and D. Isaak (2006), Mapping and monitoring stream aquatic habitat with a narrow-beam green lidar (EAARL), *Eos Trans. AGU*, *86*(52), Fall Meet. Suppl., Abstract H34B-05.

McKean, J., D. Isaak, and C. W. Wright (2008), Geomorphic controls on salmon nesting patterns described by a new, narrow-beam terrestrial-aquatic lidar, *Frontiers Ecol. Environ.*, *6*(3), 125–130.

McKean, J. A., D. Nagel, D. Tonina, P. Bailey, C. W. Wright, C. Bohn, and A. Nayegandhi (2009), Remote sensing of channels and riparian zones with a narrow beam aquatic-terrestrial LIDAR, *Remote Sens.*, *1*, 1065–1096.

Meehan, W. R. (1974), The forest ecosystem of southeast Alaska: Fish habitats, *Gen. Tech. Rep.*, *PNW-GTR-15*, 41 pp., Pac. Northwest Exp. Stn., U.S. Dep. of Agric. For. Serv. Portland, Oreg.

Meyer, G. A., and M. E. Leidecker (1999), Fluvial terraces along the Middle Fork Salmon River, Idaho, and their relation to glaciation, landslide dams, and incision rates: A preliminary analysis and river-mile guide, in *Guidebook to the Geology of Eastern Idaho*, edited by S. S. Hughes and G. D. Thackray, pp. 219–235, Mus. of Nat. Hist., Pocatello, Idaho.

Miller, A. J., and B. L. Cluer (1998), Modeling considerations for simulation of flow in bedrock channels, in *Rivers Over Rock: Fluvial Processes in Bedrock Channels*, Geophys. Monogr. Ser., vol 107, edited by K. J. Tinkler and E. E. Wohl, pp. 61–104, Washington, D. C.

Montgomery, D. R., J. M. Buffington, N. P. Peterson, D. Schuett-Hames, and T. P. Quinn (1996), Stream-bed scour, egg burial depths, and the influence of salmonid spawning on bed surface mobility and embryo survival, *Can. J. Fish. Aquat. Sci.*, *53*, 1061–1070.

Morgan, P., E. K. Heyerdahl, and C. E. Gibson (2008), Multi-season climate synchronized widespread forest fires throughout the 20th-century, Northern Rockies, USA, *Ecology*, *89*, 717–728.

Morvan, H., D. Knighton, N. Wright, X. Tang, and A. Crossley (2008), The concept of roughness in fluvial hydraulics and its formulation in 1D, 2D and 3D numerical simulation models, *J. Hydraul. Res.*, *46*(2), 191–208.

Mote, P. W., et al. (2003), Preparing for climatic change: The water, salmon, and forests of the Pacific Northwest, *Clim. Change*, *61*, 45–88.

Mote, P. W., A. F. Hamlet, M. P. Clark, and D. P. Lettenmaier (2005), Declining mountain snowpack in western North America, *Am. Meteorol. Soc.*, *86*, 39–49.

Mueller, E. R., J. Pitlick, and J. M. Nelson (2005), Variation in the reference Shields stress for bed load transport in gravel-bed streams and rivers, *Water Resour. Res.*, *41*, W04006, doi:10.1029/2004WR003692.

Naiman, R. J., J. J. Latterell, N. E. Pettit, and J. D. Olden (2008), Flow variability and the biophysical vitality of river systems, *C. R. Geosci.*, *30*, 629–643.

Nelson, J. M., and R. R. McDonald (1997), Mechanics and modeling of flow and bed evolution in lateral separation eddies, Glen Canyon Environmental Studies Report, 69 pp., Grand Canyon Monit. and Res. Cent., Flagstaff, Ariz.

Nelson, J. M., and J. D. Smith (1989), Flow in meandering channels with natural topography, in *River Meandering*, *Water Resour. Monogr. Ser., vol. 12*, edited by S. Ikeda and G. Parker, pp. 69–102, AGU, Washington, D. C.

Nelson, J. M., S. J. Bennett, and S. M. Wiele (2003), Flow and sediment transport modeling, in *Tools in Fluvial Geomorphology*, edited by G. M. Kondolf and H. Piegay, pp. 539–576, John Wiley, New York.

Nicholas, A. P., and C. A. Mitchell (2003), Numerical simulation of overbank processes in topographically complex floodplain environments, *Hydrol. Processes*, *17*, 727–746.

Parker, G. (1979), Hydraulic geometry of active gravel rivers, *J. Hydraul. Div. Am. Soc. Civ. Eng.*, *105*(HY9), 1185–1201.

Parker, G., and P. C. Klingeman (1982), On why gravel bed streams are paved, *Water Resour. Res.*, *18*, 1409–1423.

Parker, G., S. Dhamotharan, and H. Stefan (1982), Model experiments on mobile, paved gravel bed streams, *Water Resour. Res.*, *18*, 1395–1408.

Pasternack, G. B. (2011), *2D Modeling and Ecohydraulic Analysis*, 158, pp., Univ. California at Davis, Davis, Calif.

Pasternack, G. B., and A. Senter (2011), 21st century instream flow assessment framework for mountain streams, 399 pp., Public Interest Energy Res., Calif. Energy Comm, Davis, Calif.

Pasternack, G. B., A. T. Gilbert, J. M. Wheaton, and E. M. Buckland (2006), Error propagation for velocity and shear stress prediction using 2D models for environmental management, *J. Hydrol.*, *328*, 227–241.

Pederson, G. T., S. T. Gray, C. A. Woodhouse, J. L. Betancourt, D. B. Fagre, J. S. Littell, S. Watson, B. H. Luckman, and L. J. Graumlich (2011), The unusual nature of recent snowpack declines in the North American Cordillera, *Science*, *333*, 332–335.

Pitlick, J. (1994), Relation between peak flows, precipitation, and physiography for five mountainous regions in the western USA, *J. Hydrol.*, *158*, 219–240.

Pupacko, A. (1993), Variations in northern Sierra Nevada streamflow: Implications of climate change, *J. Am. Water Res. Assoc.*, *29*(2), 283–290.

Quinn, T. P. (2005), *The Behavior and Ecology of Pacific Salmon and Trout*, Am. Fish. Soc., Bethesda, Md.

Regonda, S., B. Rajagopalan, M. Clark, and J. Pitlick (2005), Seasonal cycle shifts in hydroclimatology over the western United States, *J. Clim.*, *18*, 372–384.

Richards, K. (1990), Fluvial geomorphology: Initial motion of bed material in gravel-bed rivers, *Prog. Phys. Geogr.*, *14*, 395–415.

Rieman, B., and D. Isaak (2010), Climate change, aquatic ecosystems and fishes in the Rocky Mountain West: Implications and alternatives for management, *Gen. Tech. Rep. RMRS-GTR-250*, 46 pp., Rocky Mountain Res. Stn., U.S. Dep. of Agric. For. Serv., Fort Collins, Colo.

Ryan, S. E., and W. W. Emmett (2002), The nature and flow of sediment transport in Little Granite Creek near Bondurant, Wyoming, *Gen. Tech. Rep. RMRS-GTR-90*, 48 pp., Rocky Mountain Res. Stn., U.S. Dep. of Agric. For. Serv., Fort Collins, Colo.

Ryan, S. E., and C. A. Troendle (1996), Bedload transport patterns in coarse-grained channels under varying conditions of flow. in *Proc. Sixth Federal Interagency Sedimentation Conf.*, March 10–14, 1996, Las Vegas, Nev., pp. VI-22 to VI-27b, Federal Energy Regulatory Commission, Washington, D.C.

Schmidt, D. L., and J. H. Mackin (1970), Quaternary geology of Long and Bear Valleys, west-central Idaho, *U.S. Geol. Surv. Bull.*, *1311-A*.

Schuett-Hames, D. E., N. P. Peterson, R. Conrad, and T. P. Quinn (2000), Patterns of gravel scour and fill after spawning by chum salmon in a western Washington stream, *N. Am. J. Fish. Manage.*, *20*, 610–617.

Seegrist, D. W., and R. Gard (1972), Effects of floods on trout in Sagehen Creek, California, *Trans. Am. Fish. Soc.*, *101*, 478–482.

Stewart, I. T. (2009), Changes in snowpack and snowmelt runoff for key mountain regions, *Hydrol. Processes*, *23*, 78–94.

Stewart, I. T., D. R. Cayan, and M. D. Dettinger (2004), Changes in snowmelt runoff timing in western North America under a 'business as usual' climate change scenario, *Clim. Change*, *62*, 217–232.

Stewart, I. T., D. R. Cayan, and M. D. Dettinger (2005), Changes toward earlier streamflow timing across western North America, *J. Clim.*, *18*, 1136–1155.

Thurow, R. F. (2000), Dynamics of Chinook salmon populations within Idaho's Frank Church Wilderness: Implications for persistence, in *Proceedings of the Wilderness Science in a Time of Change Conference*, *RMRS-P-15-Vol-3*, pp. 143–151, Rocky Mountain Res. Stn., U.S. Dep. of Agric. For. Serv., Fort Collins, Colo.

Tonina, D., and J. A. McKean (2010), Climate change impact on salmonid spawning in low-gradient streams in central Idaho, USA, in *Proceedings of the 9th International Conference on Hydroinformatics*, *Sept. 7–10,*

Tianjin, China, edited by J. Tao et al., pp. 389–397, Chem. Ind. Press, Beijing.

Tonina, D., C. H. Luce, B. Rieman, J. M. Buffington, P. Goodwin, S. R. Clayton, S. M. Ali, J. J. Barry, and C. Berenbrock (2008), Hydrological response to timber harvest in northern Idaho: Implications for channel scour and persistence of salmonids, *Hydrol. Processes*, *22*(17), 3223–3235.

Tonina, D., J. McKean, C. Tang, and P. Goodwin (2011), New tools for aquatic habitat modeling, in *Proceedings of the 34th IAHR World Congress*, *26 June to 1 July 2011, Brisbane, Australia*, pp. 3137–3144.

Torizzo, M., and J. Pitlick (2004), Magnitude-frequency of bed load transport in mountain streams in Colorado, *J. Hydrol.*, *290*, 137–151.

Waples, R. S., G. R. Pess, and T. Beechie (2008), Evolutionary history of Pacific salmon in dynamic environments, *Evol. Appl.*, *189–206*, doi:10.1111/j.1752-4571.2008.00023.x.

Westerling, A. L., H. G. Hidalgo, D. R. Cayan, and T. W. Swetnam (2006), Warming and earlier spring increases western U.S. forest wildfire activity, *Science*, *313*, 940–943.

Whiting, P. J., and W. E. Dietrich (1991), Convective accelerations and boundary shear stress over a channel bar, *Water Resour. Res.*, *27*(5), 783–796.

Wilcock, P. R., and B. T. DeTemple (2005), Persistence of armor layers in gravel-bed streams, *Geophy. Res. Lett.*, *32*, L08402, doi:10.1029/2004GL021772.

Wilcock, P. R., and B. W. McArdell (1993), Surface-based fractional transport rates: Mobilization thresholds and partial transport of a sand-gravel sediment, *Water Resour. Res.*, *29*, 1297–1312.

Wilcock, P. R., and B. W. McArdell (1997), Partial transport of a sand-gravel sediment, *Water Resour. Res.*, *33*, 233–245.

Yarnell, S. M., J. H. Viers, and J. F. Mount (2010), Ecology and management of the spring snowmelt recession, *Bioscience*, *60*, 114–127.